Inversion of the Slip Distribution of an Earthquake From InSAR Phase Gradients: Examples Using Izmit Case Study

Alessandro Parizzi

***Abstract*— This letter investigates the estimation of the slip distribution of a seismic event using the information provided by interferometric phase gradients. Even if the technique is expected to be suboptimal when compared with an estimation using the unwrapped interferometric phase, such an approach would permit to avoid the solution of phase ambiguities also including the parts of the interferogram that could not be reached by the phase unwrapping otherwise. This specifically addresses the cases where the motion gradients are so strong that particular areas have to be masked out due to unwrapping errors. Aim of this letter is to propose a possible way to include such areas modeling the motion with phase gradients. The rationale of this letter relies on the description of the coseismic motion given by the Okada model that provides both the 3-D surface displacement and the gradient tensor information. Based on the latter, this letter defines an inversion strategy that uses the information extracted by the phase gradients, hence avoiding phase unwrapping. This technique is tested on real test sites and compared with the results obtained using the absolute phase.**

***Index Terms*— Differential SAR interferometry, fault modeling, frequency estimation, gradient tensor.**

I. Introduction

THE phase unwrapping is the main limitation factor for the exploitation of the repeat-pass interferometry. The presence of noise and the strong deformation gradients can, in fact, lead to a wrong interpretation of the phase ambiguities and, consequently, the generation of errors that propagates in space. Such errors are particularly hard to handle since they cannot be reduced by spatial averaging. This problem is an issue in applications working with the geophysical modeling of a single interferometric pair. A possible solution, where a modeling of tectonic fault is carried out by directly using the wrapped interferometric phase, has been proposed in [1] and [2]. This avoids, of course, the phase unwrapping, but it has the drawback of having non-Gaussian distributed misfits [1]. Therefore, the inversion of the system implies the choice of the proper ambiguity band that fits the model, making the problem anyway similar to a phase unwrapping. The idea of using the phase gradients to interpret the geophysical phenomena was, hence, often considered [3], [4]. This should extend the spatial range of exploitation of the SAR interferograms since it permits to include also isolated spots of the coherent phase. However, the interpretation of a phenomena using its derivatives has the drawback of filtering its high-pass component only [3]. This results in a significant reduction of the SNR since small scales of natural phenomena contain, in general, less signal. Nonetheless, in case of strong motions compared to the radar wavelength, the gradients SNR is acceptable, and such information can be important, especially in areas that cannot be reached due to the unwrapping errors.

Ali and Feigl [5] modeled the displacement induced by volcanic activity using interferometric phase gradients. This letter investigates the use of phase gradients also for fault slip distribution inversion. The aim is to keep a methodological point of view, focusing the attention mainly on the remote sensing aspects. In Sections II and III, the problem is defined from the radar measurement point of view, and in Section IV, it is then applied to real data. In order to discuss the methodology, a particular example has been chosen. The ERS interferogram of the Izmit earthquake is a typical case, where the phase unwrapping can critically influence the results [2], and hence, it has been analyzed in this letter. The approach has been applied to the data, and the results are compared with the results obtained using the absolute phase, discussing them in the light of the theoretical expectations.

II. InSAR Phase Gradients' Measurements

The key feature of the technique is the possibility of estimating phase gradients directly from the wrapped interferometric phase. The problem can be seen in different ways. The point of view of this letter is to see the deformation gradients as proportional to the main local fringe frequency since the frequency is, by definition, the derivative of the phase. The gradient measurements $\vec{\nabla}\phi_k$ can be, hence, estimated from the single-look complex data performing a frequency estimation. Multilooking and subsampling are anyhow implicit in the fringe frequency estimation since the computation is done windowwise. Nevertheless, this allows theoretically identifying the gradients that would not be any more visible at the multilooked interferogram level due to the resolution reduction. Being (r, a) the range and azimuth coordinates in radar geometry, the interferogram is a complex number $z(r, a)$. Considering the interferometric phase varying by several wavelengths within the scale of the

Manuscript received June 10, 2018; revised August 1, 2018, October 24, 2018, and March 7, 2019; accepted March 29, 2019. Date of publication May 15, 2019; date of current version October 30, 2019. This work was supported by Helmoltz Alliance Remote Sensing and Earth System Dynamics.

The author is with the Remote Sensing Technology Institute, German Aerospace Center (DLR), 82234 Weßling, Germany (e-mail: alessandro.parizzi@dlr.de).

Digital Object Identifier 10.1109/LGRS.2019.2909025

deformation pattern, it is possible to perform a local linear approximation of the deformation phase. Hence, in a given point (r_0, a_0), the phase of the interferogram $z = Ae^{j\phi}$ can be substituted by its first-order Taylor approximation

$$\phi \approx \frac{4\pi}{\lambda}\left(\frac{\partial \delta_s}{\partial r}(r - r_0) + \frac{\partial \delta_s}{\partial a}(a - a_0)\right) + \phi_0 \tag{1}$$

where A is the product of master and slave reflectivity and $\delta_s = \boldsymbol{\delta}^T \boldsymbol{s}$ is the projection of the displacement vector $\boldsymbol{\delta}$ along the line of sight (LoS) $\boldsymbol{s}$. It is worth to point out that the complexity of the deformation patterns could require a local adapting of the dimension of the estimation window in order to make the first-order Taylor approximation reasonable [5]. The optimal estimation of the phase gradients is, in general, not trivial since the complex SAR interferograms cannot be considered simply as an ideal complex sinusoid. For very high gradients, the effect of the wavenumber shift has to be taken into account as in [6]. However, for moderate gradients, the approximation holds and periodogram can be used [7].

III. Problem Inversion Using Gradient Tensor

Being (e, n, v) the reference system oriented in accordance with the local east, the local north, and the geodetic vertical, the change in radar range can be written as the projection of the displacement vector on the sensing direction of the radar $\boldsymbol{s}$. The gradient tensor $\boldsymbol{\Psi}$ represents the derivatives of $\boldsymbol{\delta}$

$$\boldsymbol{\Psi} = \begin{bmatrix} u_{\mathrm{ee}} & u_{\mathrm{en}} & 0 \\ u_{\mathrm{ne}} & u_{\mathrm{nn}} & 0 \\ u_{\mathrm{ve}} & u_{\mathrm{vn}} & 0 \end{bmatrix}. \tag{2}$$

Radar echoes measure the projection of $\boldsymbol{\Psi}$ on the LoS at the earth's surface only; therefore, in order to satisfy the equilibrium equations, $\boldsymbol{\Psi}$ has no contributions in the column of the derivatives along the v-axis [8]. For the sake of simplicity, the notation has been shortened to $u_{ij} = \partial \delta_i / \partial j$. Hence, the displacement gradients observed in the sensing direction of the radar can be written as [9]

$$\vec{\nabla}(\boldsymbol{\delta}^T \boldsymbol{s}) = \boldsymbol{\Psi}^T \mathbf{s} = \frac{\lambda}{4\pi}\vec{\nabla}\phi. \tag{3}$$

The model proposed by Okada [10] describes the earth's surface motion generated by a seismic event both in terms of displacement and deformation (gradient tensor). Fixed the geometry of the fault, the gradient tensor $\boldsymbol{\Psi}$ derived from the Okada model can be linearized with respect to the vector of slips $\boldsymbol{\xi}$ to be estimated. Knowing the local SAR geometry from the state vectors' information, it possible to locally rotate the tensor provided by the model into radar geometry using a proper rotation matrix $\boldsymbol{T}$

$$\boldsymbol{\Theta}(\boldsymbol{\xi}) = \boldsymbol{T}^T \boldsymbol{\Psi}(\boldsymbol{\xi}) \boldsymbol{T}. \tag{4}$$

In the measurements' reference system, it is possible to write a system of equations that equate the model and measurements to be inverted, retrieving the vector of parameters $\boldsymbol{\xi}$ that are minimizing the figure of merit M

$$M = \sum_{k=0}^{N-1}\left(\frac{\lambda_k}{4\pi}\vec{\nabla}\phi - \boldsymbol{\Theta}_k(\boldsymbol{\xi})^T \mathbf{s}_k\right)^T C_{d,k}^{-1} \times \left(\frac{\lambda_k}{4\pi}\vec{\nabla}\phi - \boldsymbol{\Theta}_k(\boldsymbol{\xi})^T \mathbf{s}_k\right). \tag{5}$$

The equation system is written in general for N measurement's geometries, and $\boldsymbol{C}_{d,k}$ is the covariance matrix of the gradients of the kth geometry. Supposing that we know the statistical properties of the interferometric phase uncertainties (noise, atmosphere, and so on), it is possible to derive the covariance as the covariance of the derivative. It is worth to notice that the high-pass effect of the derivative operator drops the spatial correlation forcing the covariance function to be almost impulsive in the direction in which the derivative is applied. This means that an eventual isotropic behavior of the interferometric phase covariance function [11] will not be preserved in the gradients' covariance.

IV. Slip Distribution Inversion Using Izmit Earthquake Interferogram

The Mw 7.6 Izmit earthquake occurred on August 17, 1999, and it was the product of the right lateral strike-slip movement of a part the North Anatolian Fault [12]. Because of the E/W orientation of the fault, the coseismic displacement was very well captured by the ERS 1-2 SAR interferogram that shows a dense pattern of the azimuth-oriented interferometric fringes. The high fringe density and the temporal decorrelation (35-day interferograms) make the phase unwrapping procedure particularly prone to errors. Therefore, this case study fits very well for the investigation of a phase unwrapping-free approach. Although previous works showed the complexity of the fault [12], [13], a simplified source geometry (single fault segment) has been used, as in [2] (see Fig. 1). This is related to the scope of this letter that is aimed to focus more on methodological aspects. As a reference result for the inverted slip and its residual phase, the reader can refer to the study in [12].

The modeled fault has been divided in patches of 5×4 km along the strike and dip direction, respectively. The inversion imposes also a Laplacian as regularization ($\nabla^2 \boldsymbol{\xi} = \mathbf{0}$) to control the smoothness of the estimated slips on the fault plane [14]. In order to better discuss the feature of the gradient-based inversion of the slip distribution, the same inversion has been carried out also using the unwrapped phase.

A. Gradient Solution

The computation of the interferometric phase gradients has been performed starting from the SLCs. In order to preserve the information, no multilooking was applied in forming the interferogram. The LoS-projected component of the gradient tensor has been carried out, estimating the local fringe frequency using a periodogram. The estimation windows used was about 5×5 km, sampled at a finer grid. The estimated range and azimuth fringe frequencies are scaled to the range and azimuth LoS deformation gradients, as in (1).

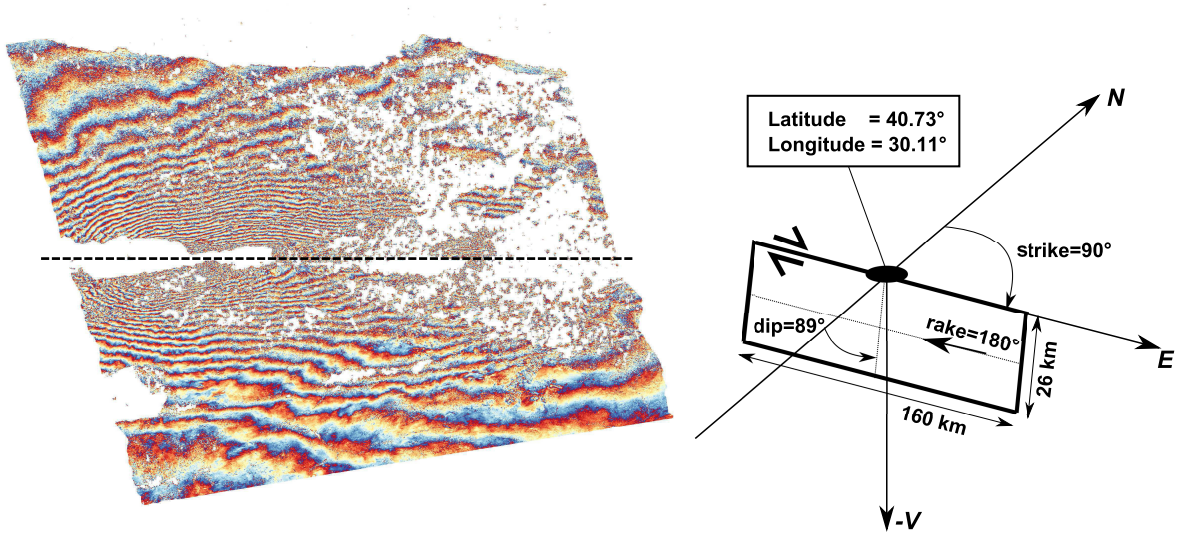

Fig. 1. Izmit earthquake displacement and geometry of the problem. (a) 35-day ERS interferogram. Black dashed line: position of the fault used in the modeling. (b) Fault geometry used for the inversion (in detail).

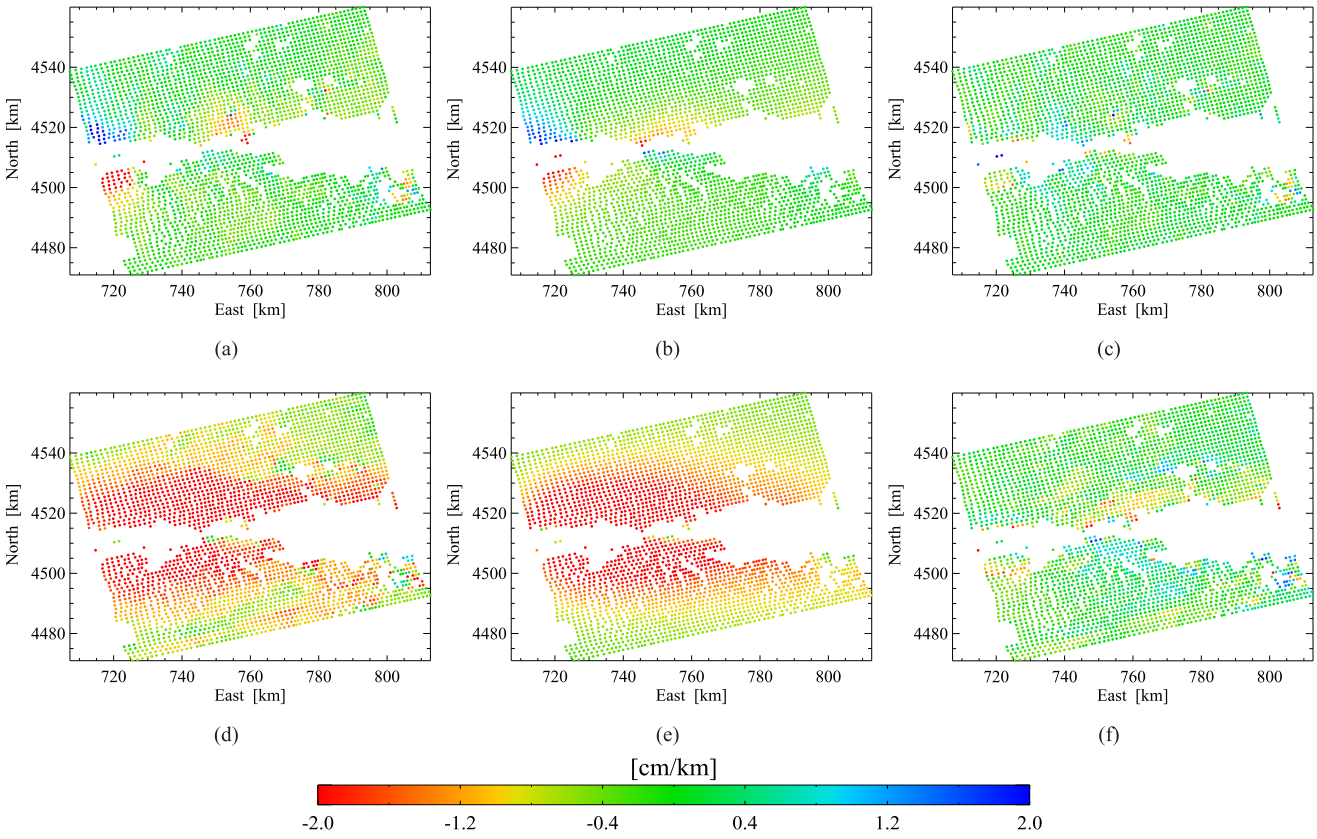

Fig. 2. Results of the gradient-based inversion. (a) and (d) Measured LoS gradients in range and azimuth, respectively. (b) and (e) Gradients modeled by the inverted slip distribution in range and azimuth, respectively. (c) and (f) Residual LoS gradients obtained, compensating the measurements with the derived model.

The direct problem is calculated using the Okada model and locally rotating the derived tensor $\boldsymbol{\Psi}(\boldsymbol{\xi})$ into radar geometry, as described in Section III. The inversion has been performed in the least square sense, forcing the vector $\boldsymbol{\xi} \geq \mathbf{0}$. The measured, modeled, and residual gradients in the range and azimuth direction are shown in Fig. 2.

B. Unwrapped Phase Solution

In order to compare the previously derived results, the inversion has been also carried out using the unwrapped interferometric phase. A coherence mask having 0.18 threshold has been over imposed in order to keep the phase error in a reasonable range. The extracted points have been unwrapped

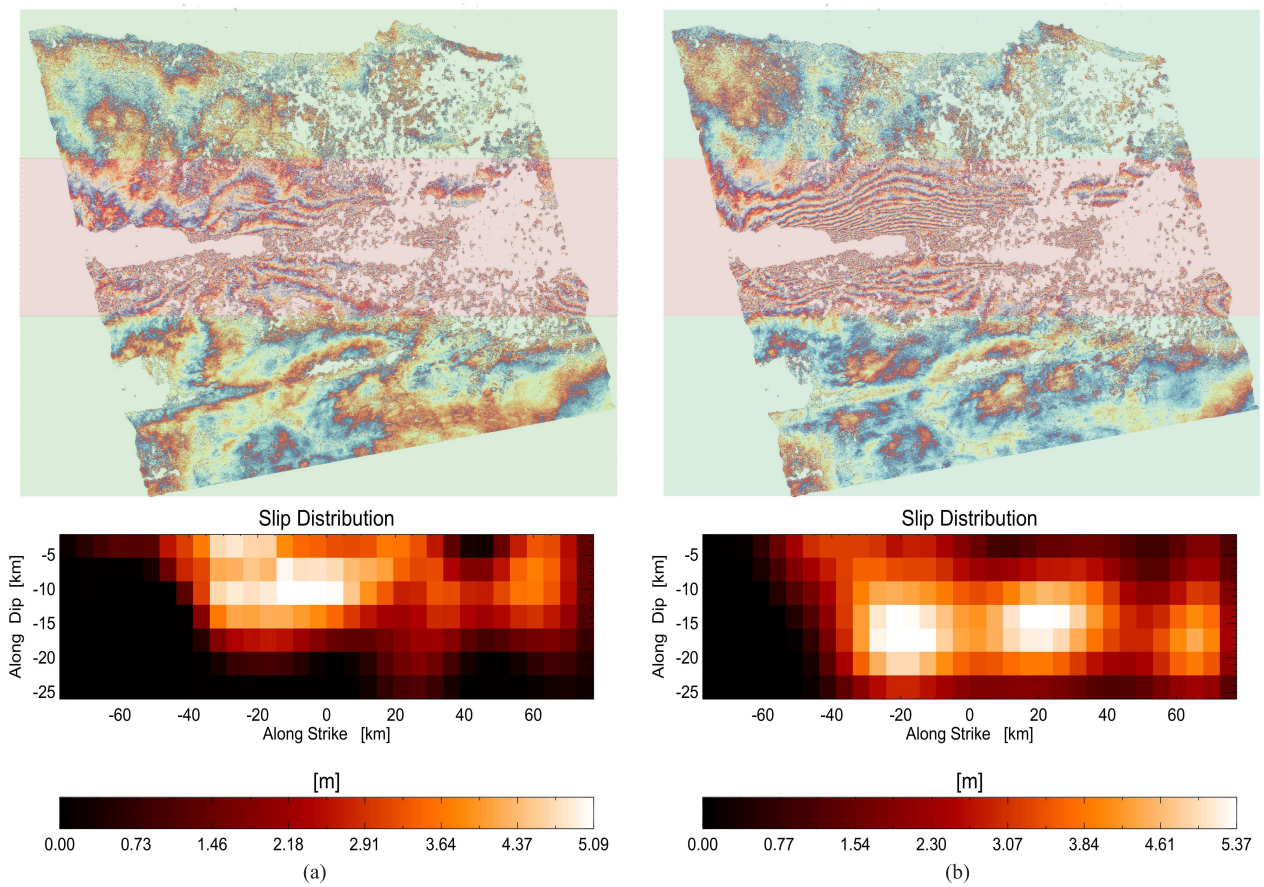

Fig. 3. Results comparison. (a) Wrapped residual interferogram and slip distribution over the fault plane for the gradient solution. (b) Wrapped residual interferogram and slip distribution over the fault plane for the unwrapped phase solution. The reshaded area is aimed to highlight the area closer to the fault, where the unwrapping errors are more likely to occur.

using a sparse grid minimum cost flow (MCF) [15]. Due to the fact that the whole scene is crossed by the tectonic fault, critical unwrapping errors have been avoided unwrapping the scene in two separate "tiles": one covering the area north of the fault and the other covering the southern area. Two reference points have set close to the northwest corner of the interferogram and the southwest corner, respectively. In this case, the direct problem is designed, describing the projection of the displacement generated by the Okada model in LoS calibrated to the displacement generated by the Okada model in LoS in the reference point. The absolute phases of the two tiles have been jointly inverted, obtaining a parameter vector $\boldsymbol{\xi}_{\phi}$ comparable to the one obtained using the gradients ($\boldsymbol{\xi}_{\Delta}$).

C. Discussion

In order to fairly compare the obtained results, the residuals displayed in the wrapped interferometric phase have been used. The modeled phase corresponding to the inverted results has been computed, wrapped, and used to compensate for the original interferogram. In this way, it is possible to visually evaluate the capability of the inverted models to explain the interferometric measurement. Unwrapped phase provides higher sensitivity to deformation, as expected from the theory. This is visible far away from the fault (highlighted in green dots in Fig. 3), where the interferometric phase is better compensated by the model derived from the unwrapped phase. However, close to the fault (highlighted in red dots in Fig. 3), the solution obtained using gradients is considerably better. Here, the deformation pattern generates strong phase gradients that compromise the success of the phase unwrapping. However, the gradients' measurements are able to provide an ambiguity-free information that can be more easily inverted in a least square sense despite their noisy nature.

Both inversions have been almost identically regularized so that the two inverted slip distributions, $\boldsymbol{\xi}_{\phi}$ and $\boldsymbol{\xi}_{\Delta}$, present the same spatial smoothness [14]. The two slip distributions, $\boldsymbol{\xi}_{\phi}$ $\boldsymbol{\xi}_{\Delta}$, present a similar spatial pattern although shifted on the fault plane along the dip direction. This can be interpreted, considering the relation between the depth of the slip and the scale of the corresponding surface deformation (the deeper the motion is, the more low pass the surface deformation is) [8]. Therefore, since the gradients' measurements are limited in observing the high-pass part of the motion, the maximum observable depth results are also to be limited accordingly.

V. Conclusion

This letter has discussed and shown the possibility of using the interferometric phase gradients in slip distribution inversion. Although the use of such measurements is inherently suboptimum, their robustness to unwrapping error is an interesting

feature that helps in fully exploiting the interferometric phase information. In line with the theory, the results discussed in this letter show how the absolute interferometric phase is performing, in general, better. However, this statement has been proven to be true only in the case of a correct solution of the phase ambiguities, as it happened far away from the fault, where the motion gradients are small (see Fig. 3). The unwrapping errors due to high fringe rate in the proximity of the fault lead to an underestimation of the motion in this area and, consequently, to a different interpretation of the motion in terms of the fault slip (see Fig. 3). The gradient-based solution, on the other side, proved to be more robust, being able to better compensate the interferometric phase close to the fault. Therefore, one could think of a synergistic use of phase gradients that can help mitigating the unwrapping-related problems. Some possible applications include the integration with cross correlation (the shifts catching the low pass part of the motion, the gradients the high pass one), the improvement of the data coverage (including areas where the phase unwrapping is bound to fail), or the estimation of an *a priori* solution that can be used to properly unwrap the interferogram.

REFERENCES

[1] K. L. Feigl and C. H. Thurber, "A method for modelling radar interferograms without phase unwrapping: Application to the M 5 Fawnskin, California earthquake of 1992 December 4," *Geophys. J. Int.*, vol. 176, no. 2, pp. 491–504, Feb. 2009.

[2] G. Fornaro, S. Atzori, F. Calo, D. Reale, and S. Salvi, "Inversion of wrapped differential interferometric SAR data for fault dislocation modeling," *IEEE Trans. Geosci. Remote Sens.*, vol. 50, no. 6, pp. 2175–2184, Jun. 2012.

[3] D. T. Sandwell and E. J. Price, "Phase gradient approach to stacking interferograms," *J. Geophys. Res.*, vol. 103, no. B12, pp. 30183–30204, Dec. 1998.

[4] A. Sharov, "Gradient approach to InSAR modelling of glacial dynamics and morphology," in *Proc. 22nd EARSeL Symp.* Rotterdam, The Netherlands: Mill Press, 2003, pp. 373–381.

[5] S. T. Ali and K. L. Feigl, "A new strategy for estimating geophysical parameters from InSAR data: Application to the Krafla central volcano in Iceland," *Geochem., Geophys. Geosyst.*, vol. 13, no. 6, Jun. 2012.

[6] A. M. Guarnieri and S. Tebaldini, "ML-based fringe-frequency estimation for InSAR," *IEEE Geosci. Remote Sens. Lett.*, vol. 7, no. 1, pp. 136–140, Jan. 2010.

[7] S. Kay and R. Nekovei, "An efficient two-dimensional frequency estimator," *IEEE Trans. Acoust., Speech Signal Process.*, vol. 38, no. 10, pp. 1807–1809, Oct. 1990.

[8] P. Segall, *Earthquake and Volcano Deformation*. Princeton, NJ, USA: Princeton Univ. Press, 2010.

[9] A. Parizzi and W. A. Jaber, "Estimating strain and rotation from wrapped SAR interferograms," *IEEE Geosci. Remote Sens. Lett.*, vol. 15, no. 9, pp. 1367–1371, Sep. 2018.

[10] Y. Okada, "Surface deformation due to shear and tensile faults in a half-space," *Bull. Seismol. Soc. Amer.*, vol. 75, no. 4, pp. 1135–1154, Aug. 1985.

[11] S. Knospe and S. Jonsson, "Covariance estimation for dInSAR surface deformation measurements in the presence of anisotropic atmospheric noise," *IEEE Trans. Geosci. Remote Sens.*, vol. 48, no. 4, pp. 2057–2065, Apr. 2010.

[12] Z. Çakir, J.-B. de Chabalier, R. Armijo, B. Meyer, A. Barka, and G. Peltzer, "Coseismic and early post-seismic slip associated with the 1999 Izmit earthquake (Turkey), from SAR interferometry and tectonic field observations," *Geophys. J. Int.*, vol. 155, no. 1, pp. 93–110, 2003. doi: 10.1046/j.1365-246X.2003.02001.x.

[13] T. Wright, E. Fielding, and B. Parsons, "Triggered slip: Observations of the 17 August 1999 Izmit (Turkey) Earthquake using radar interferometry," *Geophys. Res. Lett.*, vol. 28, no. 6, pp. 1079–1082, Mar. 2001.

[14] S. Jonsson, H. Zebker, P. Segall, and F. Amelung, "Fault slip distribution of the 1999 Mw 7.1 hector mine, california, earthquake, estimated from satellite radar and GPS measurements," *Bull. Seismological Soc. Amer.*, vol. 92, no. 4, pp. 1377–1389, May 2002.

[15] M. Costantini, "A novel phase unwrapping method based on network programming," *IEEE Trans. Geosci. Remote Sens.*, vol. 36, no. 3, pp. 813–821, May 1998.